Contents lists available at ScienceDirect

Radiation Physics and Chemistry

journal homepage: http://ees.elsevier.com

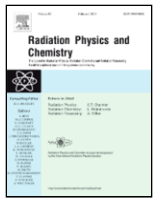

Radiation dose assessment of 64 Multi-Slices Computed Tomography scanner

R.S. Omar [a,*], S. Hashim [a,b], S.K. Ghoshal [a], D.A. Bradley [c], N.D. Shariff [d]

[a] Department of Physics, Faculty of Science, Universiti Teknologi Malaysia, 81310, Johor Bahru, Malaysia
[b] Centre for Sustainable Nanomaterials (CSNano), Ibnu Sina Institute for Scientific and Industrial Research (ISI-SIR), Universiti Teknologi Malaysia, 81310, UTM Skudai, Johor, Malaysia
[c] Center of Biomedical Physics, School of Healthcare and Medical Sciences, Sunway University, Malaysia
[d] Hospital Sultanah Aminah, Johor Bahru, 80100, Malaysia

ARTICLE INFO

Keywords
CTDI
MDCT
PMMA phantom

ABSTRACT

This paper reports the performance and dose assessment of the X-ray generator and CT dosimetry of 64 Multi-Slices Computed Tomography (MSCT) scanners operating under the CT scanning condition during the axial mode. The dose was evaluated at various parameters (kV, mA, and exposure time) using a multi-function detector (Unfors) and nanoDot™ optically stimulated luminescence dosimeters (OSLDs). The measured values of the weighted CT Dose Index ($CTDI_w$) were obtained using a 100 mm standard pencil beam ion chamber and nanoDot™ OSLDs operated on a cylindrical PMMA phantom of 160 mm long (160 mm-diameter head and 320 mm-diameter). The $CTDI_w$ values were specified either according to the central axis or 10 mm from the 4 outer edges of the phantom. The two sizes of the phantoms based on the measurements of the $CTDI_w$ of the CT scanner were recorded. The values of $CTDI_w$ were calculated to determine the performance of the CT X-ray generator. The deviation accuracy of the tube voltage was ± 5 kV or $\pm 5\%$ (whichever is greater) whereas the accuracy of the tube potential (mA) was $\pm 10\%$. The execution of the CT dosimetry steps was shown to ensure patient safety with reduced risk during the improper selection of the dose. It is established that the measured $CTDI_w$ values for the radiation dosage under exceptional CT scanning conditions in the axial mode may enable to meet the manufacturer's guidelines ($< \pm 20\%$).

1. Introduction

The X-ray radiation can be outlined as composed of x-rays or a form of electromagnetic (EM) radiation. Due to their penetrating capability, hard x-rays are widely used to image the internal of objects and normally in medical radiography which includes medical computed tomography (CT), x-ray crystallography, mammography, and airport security. Using comparison, soft x-rays are easily absorbed in the air; the attenuation length of 600 eV (~2 nm) x-rays in water is less than 1 μm (μm). There is no consensus for a definition distinguishing between x-rays and gamma rays. One common practice is to differentiate between the two types of radiation primarily based on their source. In this situation, x-rays are emitted via electrons, whilst gamma rays are emitted through the atomic nucleus (Dendy and Heaton, 2011; Feynman et al., 2013). A CT scan, additionally known as a CAT (computed axial tomography) scan, is a specialized x-ray test. X-ray CT is a non-destructive method to acquire a 3-dimensional (3D) information and images of interior features inside solid objects. The denser the tissue, the less x-rays pass through. Despite that, a CT scan can be carried out on any section of the head or body. Complications from CT scans are rare. Rarely, a few people have a hypersensitivity to the dye (contrast agent) that is sometimes used. This can be treated without delay. Very rarely, the dye may additionally cause a few kidney harms, most commonly in people already recognized to have kidney problems. In precaution, if viable, pregnant ladies should not have a CT scan, as there is a small risk that x-rays may cause an abnormality to the unborn child. This is due to the fact, CT scans use x-rays, which is a sort of radiation. Exposure to large doses of radiation is linked to growing cancer or leukaemia (regularly many years later).

Numerous studies have aimed to estimate the chance of growing cancer or leukaemia following a CT scan (Brenner and Hall, 2012; Pearce et al., 2012; De Gonzalez et al., 2016; Cohen, 2015). The chance of harm from the dose of radiation used in CT scanning is a concept to be very small, but it is not absolutely without risk. Most of the time, “the higher the dose of radiation, the greater the risk”. For instance, the bigger the part of the body scanned, the more the radiation dose. A repeat CT scans through the years cause a general increase of dose. Additionally, the younger the patient having a CT scan, the greater the lifetime risk of developing cancer or leukaemia. In many situations, the benefit of a CT scan substantially outweighs the risk. How-

* Corresponding author.
E-mail address: ratnasuffhiyanni@gmail.com (R.S. Omar)

https://doi.org/10.1016/j.radphyschem.2020.108904
Received 14 March 2020; Received in revised form 28 March 2020; Accepted 30 March 2020
Available online xxx
0969-806/

ever, as the identical study concludes, even though medical benefits should outweigh the small absolute risks, radiation doses from CT scan thought to be kept as low as possible and alternative approaches, which do not involve ionizing radiation, should be taken into consideration if appropriate. Because of the small risk, the Committee on Medical Aspects of Radiation in the Environment (COMARE) has recommended that routine whole-body CT scans should not be offered to people without signs and symptoms as a part of fitness assessments.

The CT protocol optimization, quality controls of CT scanners and accurate evaluation of radiation dose have to turn out to be an urgent task in the control in CT exposures. Even though MOSFET detectors can offer real-time readout functionality, the total number of simultaneous dose measurements is restrained by the electronic probes. In contrast, thermoluminescence dosimeter (TLD) and optically stimulated luminescence dosimeter (OSLD) are higher desirables for acquiring densely sampled dose maps. The merits, negative aspects, as well as advantages of TLD and OSLD, have been mentioned in the literature (McKeever and Moscovitch, 2002). The OSL dosimetry device has gained increasing popularity in the medical physics discipline, included the microStar reader (Landauer Inc., Glenwood, IL) and InLight® nanoDot™ OSL dosimeters (Jursinic, 2007; Al-Senan and Hatab, 2011). Experimental dose measurements are frequently accomplished using anatomical physical phantoms that are designed to allow small dosimeters to be located at various locations corresponding to organs (Xu and Eckerman, 2009). Such dose measurements take into account the have an impact on of patient-particular tube current or voltage modulation techniques and are consequently more accurate than techniques using simple phantoms inclusive of a cylinder or a slab. It must be also noted that CT scanners protocol are generally affecting the dose distribution and radiation dose toward patient or phantom. CT scanners are being increasingly more utilized by radiotherapy departments for image acquisition for treatment making plans purposes (Mutic et al., 2003), similarly to the conventional roles of patient diagnosis and most cancers staging. In this point of view, two CT parameters should be noted by clinical physicists or radiographers; equipment-related factors and application-related factors (Nagel, 2007). This placing further crucial needs on scanner overall performance necessities and quality control processes. Consequently, in this study, we reported the performance of an X-ray generator and the CT dosimetry of a 64-MSCT scanner operating under CT scanning condition during the axial mode. The scan is performed via a standard quality control (QC) Unfors detector and nanoDot™ OSLDs. The measurement of weighted CT Dose Index ($CTDI_w$) was collected using a 100 mm standard pencil beam ion chamber, and nanoDot™ OSLDs, in a 160 mm-diameter head and 320 mm-diameter body cylindrical acrylic Polymethyl-Methacrylate (PMMA) phantom (160 mm length). The $CTDI_w$ values were specified either according to the central axis or 10 mm from the 4 outer edges of the phantom. The two sizes of the phantoms based on the measurements of the $CTDI_w$ of the CT scanner were recorded. The weighted CTDIs ($CTDI_w$) were calculated and the CT X-ray generator performance observed.

2. Materials and methods

The methodology in this paper includes the microStar InLight® reader stability test, the CT X-ray generator dose measurement (in the air), and the CT dose index (CTDI) measurement (in a cylindrical acrylic Polymethyl-Methacrylate phantom). The dose measurements were collected and the results were compared using two different detectors; Unfors detector and nanoDot™ OSLDs. The measurements were assessed from CT scanner models: 64-MSCT scanner.

2.1. System calibration and stability test

Before beginning any measurements, the microStar InLight® system should be calibrated according to a specific environment. This process, for example, creating a calibration curve is extremely important as it correlates the optical response from a dosimeter to a known dose to establish the sensitivity of the system (measured in counts/dose). Fortunately, this is simple to do and the results can be stored for later use. To perform this measurement, 10–20 min waiting time should be considered for the device to warm up. At this point, it simply needs to determine if the calibration curve will be for diagnostic radiography or radiation oncology. For this study, the microStar reader is for CT application purposes. For this reason, the calibration for diagnostic radiography is applied. For virtually all diagnostic radiology users, a linear calibration is sufficient to achieve the desired level of accuracy (<10%) (Yahnke, 2009). This issue is typically encountered in diagnostic radiology were the three main applications (mammography, fluoroscopy, and CT) each use different accelerating potentials and different amounts of filtration to produce beams with the desired half-value layer (HVL) or effective energy. For reasons described above, the preferred option would be to create a set of calibration dosimeters using the appropriate reference conditions. Landauer has performed these measurements at its Glenwood Calibration Laboratory and determined them to be as listed in Table 1. This desire correction factor (0.84) information for CT application is used in this study. Using the set of calibration and quality control (QC) dosimeters supplied by Landauer, the establishment of the calibration curve the microStar InLight® system is done. These dosimeters were irradiated free-in-air using ^{137}Cs source and delivered doses ranging from 0 to 1000 mGy (100,000 mrad) covering a wider range from low to high dose level. The calibration curve is then built by analysis of the set of calibration dosimeters having doses of 0, 5, 30, 500 and 1000 mGy covering a wide range of doses from low to high dose.

Moreover, a baseline for the microStar InLight® system stability test is established before the measurement of standard dosimeter or every time before the system is used. This is because signal fluctuations within the reader may arise from different sources, including electronic noise, LED light fluctuation, PMT response and the positioning of the OSL dosimeter in the optical beam. This measurement is crucial which three positions on the measuring position dial (DRK, CAL, LED) are used to measure InLight® system stability test. These measurement standards are an important tool for monitoring reader performance. During this measurement, the adapter is removed from the unit and the dosimeter between each analysis to average out any mechanical variations in opening or positioning the dosimeter. This InLight® system stability test is repeated ten times, the mean (average), standard deviation (SD) and coefficient of variation (CoV) are computed.

2.2. Computed tomography X-ray generator dose measurement (in air measurement)

X-ray generator dose measurement was assessed via an axial scanning using 64 MSCT. The dose measurement is collected from a Unfors detector and nanoDot™ OSLDs (with a sensitivity range of 0.84–

Table 1
The microStar InLight® system correction factor (Yahnke, 2009).

Calibration Set	Mammography (~32 kVp, 0.36 mm Al HVL)	Dental (~70 kVp, ~2.4 mm Al HVL)	CT (~120 kVp, 8.4 mm Al HVL)	Cs-137 (662 keV)
80 kVp*	0.78	1.00	0.84	0.25

0.92). A 64-MSCT scanner is the latest powerful and cost-effective 7th generation model. The X-ray generator dose measurement was done using the parameters tube voltage (V), tube current (I), and exposure time (t). The assessment method for dose measurement in the air is illustrated in Fig. 1. Upon the data collection, the parameters were adjusted accordingly (Table 2) to observe the changes of the dose with a change in the respective parameter.

2.3. Computed tomography dose index measurement (PMMA head-body phantom measurement)

The CTDI dose measurement was assessed for the 64 Multi-Slices MSCT. The dose assessment was performed using the same detector type Unfors detector and nanoDot™ OSLDs. The parameters are as per the in air method (Table 2). During the data measurement, the weighted CT Dose Index ($CTDI_w$) was measured using a 100 mm standard pencil beam ion chamber and a nanoDot™ OSLDs (designed as per Fig. 3), in a 160-mm diameter head and 320-mm diameter body cylindrical acrylic Polymethyl-Methacrylate (PMMA) phantom (160 mm length). The $CTDI_w$ values were specified at the region of interest (ROI), either at the central axis (A) or 10 mm from the 4 outer edges (B, C, D, E) of the PMMA phantom, as illustrated in Fig. 2. For the $CTDI_{head}$ and $CTDI_{body}$ assessment, the 64-MSCT scanner parameters were set to 120 kV tube voltage, 350 mA tube current, 1 s exposure time, and 120 kV tube voltage, 420 mA tube current, 0.5 s exposure time, respectively. These CT parameter values were adopted from available QC test protocols.

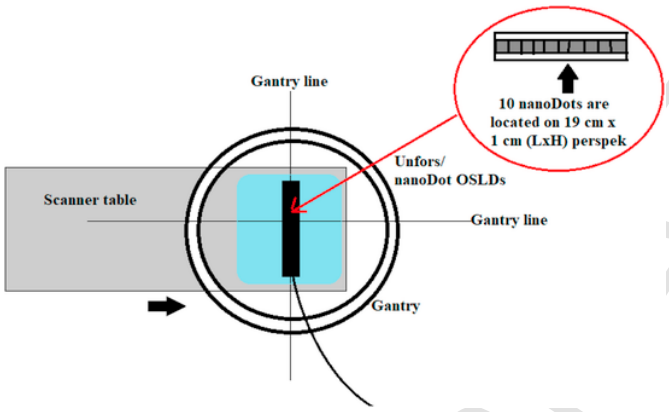

Fig. 1. The positioning of the Unfors or nanoDot™ OSLDs inside the gantry of the CT scanner where the detectors are aligned with the gantry line position.

Table 2
Parameter value adjustment for the 64-MSCT.

Parameter	Parameter value		
	Varied value	Fixed value	Constant Exposure time, t (s)
Tube Voltage, V (kV)	80	100 mA	1 s
	110	100 mA	1 s
	130	100 mA	1 s
	140	100 mA	1 s
Tube Current, I (mA)	50	120 kV	1 s
	100	120 kV	1 s
	150	120 kV	1 s
	200	120 kV	1 s
	250	120 kV	1 s
	300	120 kV	1 s

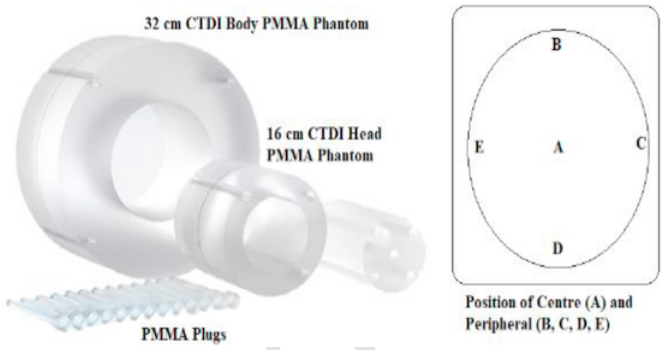

Fig. 2. The 32 cm diameter body and 16 cm diameter head PMMA phantoms with 5 regions of interest (ROIs).

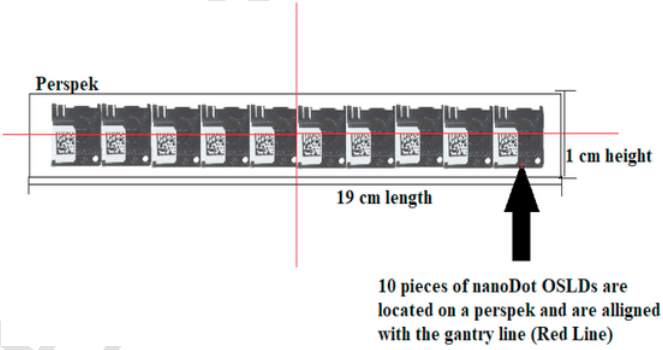

Fig. 3. The nanoDot™ OSLDs design for the $CTDI_{head}$ and the $CTDI_{body}$ assessment.

Fig. 3 illustrates a total of 10 nanoDot™ OSLDs designed so that the dosimeters could be slotted inside the PMMA phantom and aligned with the gantry's red line position during axial scanning. The dose was calculated from the average of 10 collected data.

The readout process was performed using a microStar InLight® reader. Besides, an annealing process was performed before the overall step of using the microStar Pocket Annealer (model number HA0008529). The Pocket annealer can reset the dosimeter data effectively and definitely (up to 0.1 mSv or 0.1 mGy). It also has a nearly instant reset (in less than 10 s) and is easy to use (no computer needed to reset, a simple power supply is enough). The pocket annealer is automatically delivered with the microStar pack (full version).

3. Results and discussion

3.1. MicroStar InLight® reader stability test result

The calibration curve is then built by analysis of the set of calibration dosimeters having doses of 0, 5, 30, 500 and 1000 mGy covering a wide range of doses from low to high dose. The calibration curve is presented in Fig. 4 as the dynamic range separation of the microStar InLight® reader. The curve consists of two segments that correspond to the different dose levels. As seen from Fig. 4, at doses below 100 mGy or 10,000 mrad which is referred to as “low” dose, a large amount of stimulation is required to produce a response that is separable from the noise and background. While at doses above 100 mGy (high dose), a large luminescence signal is produced with a reduced amount of stimulation. The response of the calibration curve is in agreement with the Landauer's microStar dynamic range separation (Yahnke, 2009), which shows that “strong” stimulation is needed for low doses while “weak” stimulation is required for the high dose. This curve consists of two segments, corresponding to different dose levels. The microStar InLight® reader uses a photomultiplier tube (PMT) to collect the lumi-

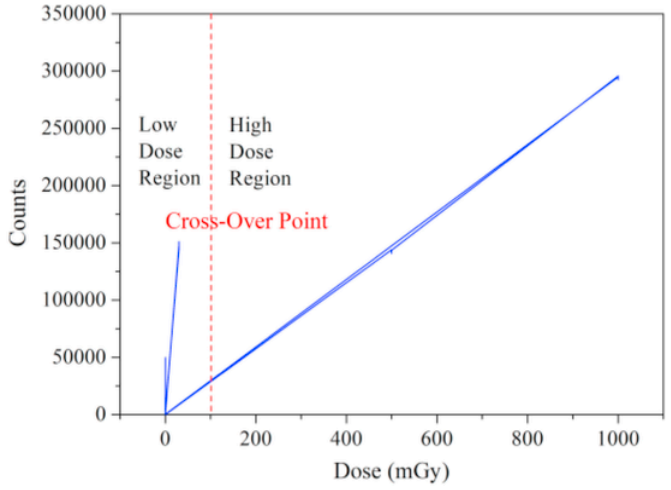

Fig. 4. Graph of reader-response of the calibrated dose (calibration curve).

nescence from an OSL dosimeter. As such, it has a finite range over which it can accurately quantify this luminescent signal. Doses at the bottom end of the dynamic range require large amounts of stimulation to respond distinguishable from background and noise while doses at the top end of the dynamic range produce an optical response that can saturate the PMT. This is graphically shown in Fig. 4 below.

The red dash vertical line indicates the cross-over point which designates the point where the microStar InLight® reader decides whether to use strong or weak stimulation. In Fig. 4., the cross-over point falls at about ~100 mGy which corresponds to the value sets by the manufacturer (Landauer, 2012). From the graph, it shows that the two levels of optical stimulation are referred to as "strong" (for doses < 100 mGy) and "weak" (for doses > 100 mGy) and is illustrated as "low dose region" and "high dose region". These correspond to "low doses" and "high doses" respectively. The terminology used, "low" and "high", is only a relative term used to characterize the amount of optical stimulation applied and is not indicative of an absolute dose.

Fig. 5 (a), (b), and (c) represent the trend analysis of the microStar InLight® reader performance test and the control limit values for DRK, CAL, and LED, respectively. The red and blue dash lines illustrate the upper limit line and lower limit line of the specific reading, respectively. This result establishes a clear criterion for determining whether or not the reader is performing at acceptable levels for this application. Aside from a warm-up period (at least 30 min), the actual test protocol takes less than 10 min to finish. The mean value of the ten successive readings for each day (counts) within 30 days represents the specified reader control limit. As shown in Fig. 4 (a), the observed maximum value of DRK was 5 ± 2 (Mean ± SD) counts, which conform with the manufacturer recommendation limit stating that DRK should be less than 30. The measured data (Mean ± SD) for CAL and LED in Fig. 5(b) and (c) were found to have an average of 1550 ± 30 and 4360 ± 151 counts, respectively. These values were within the suggested manufacturer's control limit (±10%). The presented data shows that the microStar InLight® reader performed well in this area.

3.2. CT X-ray generator dose (in air measurement) result

Fig. 6 (A) shows the measured dose distributions of the two types of detectors: the Unfors detector and nanoDot™ OSLDs in the two MSCT scanners. It shows that the dose distributions for both detectors or dosimeter types constantly increased from 80 kV to 140 kV. The nanoDot™ OSLDs measured from 10 average data points and the values recorded were not much different than the readings of the Unfors detector. The percentage difference between the nanoDot™ OSLDs and the Unfors detector for the 64 slices MSCT was 4%, −1%, −3% and −3% for 80 kV, 100 kV, 120 kV and 140 kV, respectively. According to the International Atomic Energy Agency, to meet the acceptable dose and accuracy of a potential tube, the CT X-ray generator should have a maximum deviation baseline value of ≤ ±5%. In this case, the Un-

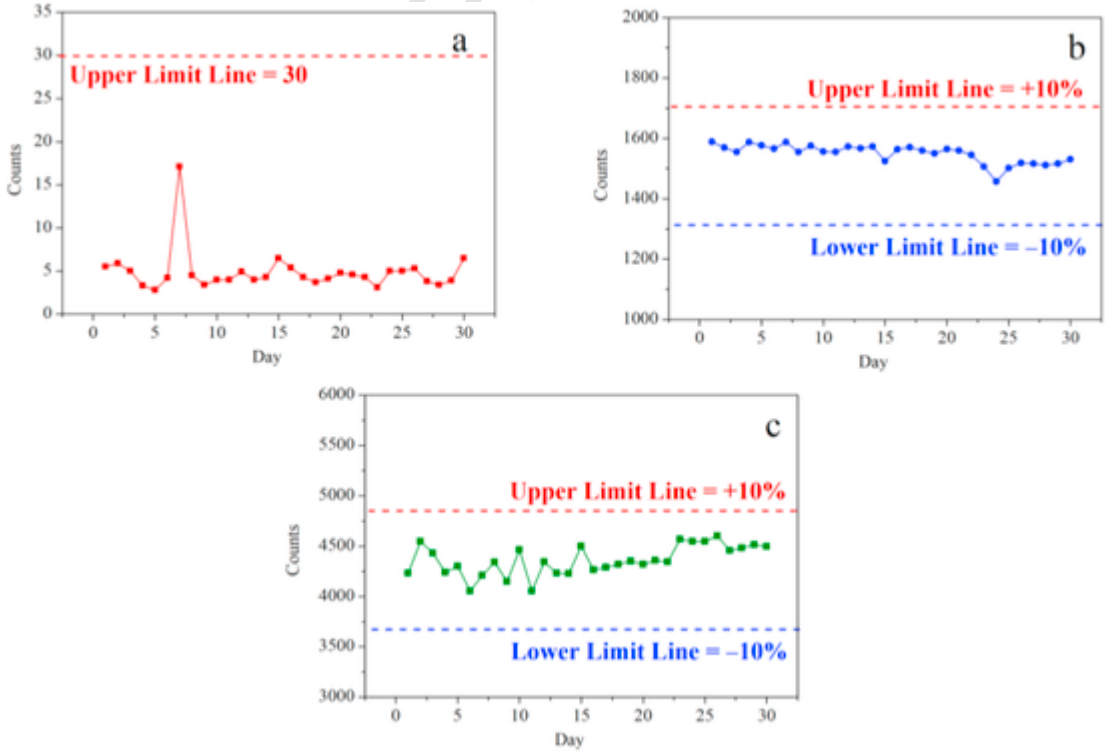

Fig. 5. PMT count values of the reader stability test for (a) dark current (DRK); (b) CAL; and (c) LED.

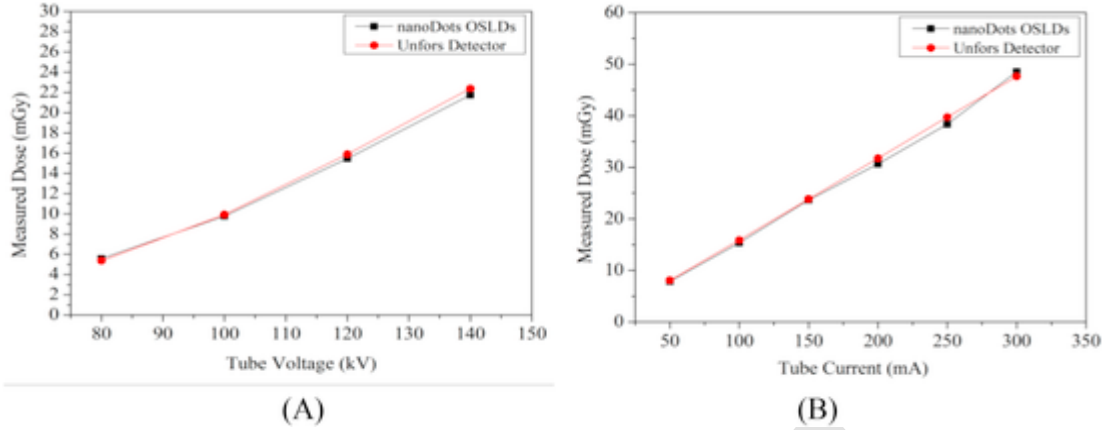

Fig. 6. A measured dose of the X-ray generator for varied values of (A) tube voltage; and (B) tube current. In both assessments, the exposure time was fixed at 1 s.

fors detector was a standardized detector. The results collected from nanoDot™ OSLDs were therefore compared to that of a Unfors detector. The results in Fig. 6 (A) show that the percentage value was ≤ ±5% for both the 64 slices MSCT X-ray generators. In terms of dose distribution, this reading was within the acceptable limit for 64 slices MSCT, as the values fell in between the manufacturer recommendations (IAEA, 2012). If the dose is extremely high, the potential tube, as well as the X-ray generator, should be investigated to determine the cause of the high dose; therefore, the patient will be prevented from being exposed to any CT risks instead of receiving benefit from the CT procedure.

Fig. 6 (B) shows the measured dose distributions from two types of detectors; the Unfors detector and nanoDot™ OSLDs in the 64 slices MSCT scanner at a minimum and maximum tube current of 50 mA and 300 mA, respectively. It can be seen from this result that the dose distribution of both detectors increased linearly with the tube current values. From the 10 mean values of the nanoDot™ OSLDs, the analysis showed that the percentage difference between the Unfors detector and nanoDot™ OSLDs was −3%, −3%, −1%, −4%, −3% and 2% for 50 mA, 100 mA, 150 mA, 200 mA, 250 mA and 300 mA, respectively, for the 64-slice MSCT. The results in Fig. 6 (B) shows the tube current percentage value at ≤ ±10% for 64-slice MSCT X-ray generators, which meet the manufacturer's recommendation (MOH, 2015). This result records the acquisition parameters, which are important to ensure that the X-ray generator has acceptable QC performance and safety; thus, exposing the patients to the lowest possible risk during the examination.

3.3. CTDI measurement dose index (PMMA head-body phantom measurement) result

The weighted CTDIs ($CTDI_w$) were calculated to determine the radiation dose for tissue under different CT scanning conditions in axial modes. The Region of interest (ROI) in Fig. 7(A) and (B) refers to the centre position (A) and peripheral position indicated by B (top), C (right), D (bottom) and E (left) on the phantom. Fig. 7(A) and (B) show that the dose distributions of the standard detector, Unfors detector and nanoDot™ OSLDs, recorded a random trend, as the detectors are located consequently from position A to E with respect to the axial modes' clockwise scanning. However, the repeated scanning from A to E for both conditions—the PMMA head and body scanning and the dose distribution of nanoDot™ OSLDs—recorded a value closed to the Unfors standard QC detector. A higher $CTDI_w$ value was recorded at the head of the PMMA phantom scanner compared to the body of the PMMA phantom scanner due to the difference in the diameter of the head and body of the phantom i.e. 160 mm and 320 mm, respectively. The dose distribution from the setting parameters of the CT protocol is influenced by the size of the phantom diameter. The smaller the phantom (or the patient in actual cases), the higher the dose delivered to the tissue or organ. In further research, the organ or tissue dose distribution should be assessed to consider the risk and benefit of CT protocols related to the patient size.

Fig. 7 (A) shows the percentage difference between the Unfors detector and nanoDot™ OSLDs, which was −5%, −7%, 3%, −9% and 2% for ROI A, B, C, D, and E, respectively, for the 64-slice MSCT 160

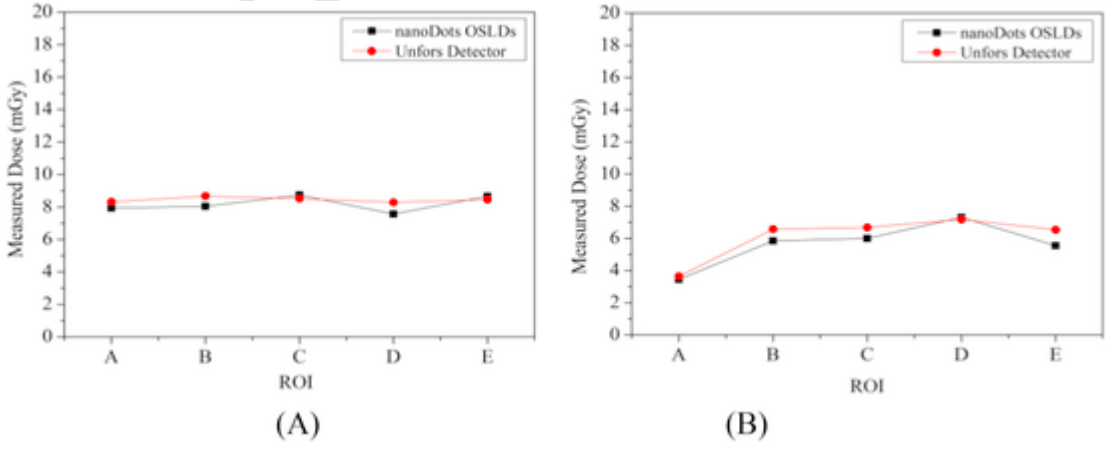

Fig. 7. Region of interest (ROI) measured dose at the (A) head and (B) body of the PMMA phantoms.

mm diameter head scanning. In Fig. 7 (B), the analysis of the 320 mm diameter body scanning recorded a percentage difference between Unfors detector and nanoDot™ OSLDs of −5%, −11%, −10%, 2% and −5% for ROI A, B, C, D, and E, respectively, in the 64 slice MSCT. These values are acceptable, as the $CTDI_{head}$ and the $CTDI_{body}$ value were ≤ ±20% of the baseline or the manufacturer's reference value. The analysis shows that in all cases of the head and body scanning, the nanoDot™ OSLDs could alternatively replace the Unfors detector for dosimetry assessment purposes in medical examinations.

4. Conclusions

The performance and dose of the X-ray generator and CT dosimetry of 64 MSCT scanners operating under the CT scanning condition were evaluated as a function of varying kV, mA, and exposure time. The radiation dosage under the special CT scanning conditions was measured in terms of $CTDI_w$ to fulfil the manufacturer's guidelines (< ±20%). The Unfors detector and nanoDot™ OSLDs were used for the radiation dose measurement on a PMMA phantom. The measured $CTDI_w$ values revealed that the nanoDot™ OSLDs can be used to replace the Unfors, indicating their similar dose detection potential for the CT scan applications. It was asserted that the performance of the 64-MSCT scans qualified the recommendation of the manufacturer. Besides, the implementation of the CT dosimetry steps ensured patient safety by reducing the future risk when the estimated dose value was improperly chosen above the relevant threshold for any routine CT examination.

Uncited references

, , .

CRediT authorship contribution statement

R.S. Omar: Writing - original draft, Conceptualization, Data curation, Formal analysis, Investigation, Methodology. **S. Hashim:** Funding acquisition, Project administration, Supervision, Validation, Methodology. **S.K. Ghoshal:** Visualization, Writing - review & editing. **D.A. Bradley:** Validation, Writing - review & editing. **N.D. Shariff:** Methodology, Resources.

Declaration of competing interest

The authors declare that they have no known competing financial interests or personal relationships that could have appeared to influence the work reported in this paper.

Acknowledgements

This work was supported by the Ministry of Education Malaysia and Universiti Teknologi Malaysia, Malaysia through Fundamental Research Grant Scheme (No. 5F222).

References

Al-Senan, R M, Hatab, M R, 2011. Characteristics of an OSLD in the diagnostic energy range. Med. Phys. 38 (7), 4396–4405.
Brenner, D J, Hall, E J , 2012. Cancer risks from CT scans: now we have data, what next? Radiology 265 (2), 330–331.
Cohen, M D, 2015. ALARA, image gently and CT-induced cancer. Pediatr. Radiol. 45 (4), 465–470.
De Gonzalez, A B, Salotti, J A, McHugh, K, Little, M P, Harbron, R W, Lee, C, Stiller, C, 2016. Relationship between paediatric CT scans and subsequent risk of leukaemia and brain tumours: assessment of the impact of underlying conditions. Br. J. Canc. 114 (4), 388.
Dendy, P P, Heaton, B, 2011. Physics for Diagnostic Radiology. third ed. CRC press, Boca Raton, FL.
Feynman, R P, Leighton, R B, Sands, M, 2013. In: The Feynman Lectures on Physics, Vol. I: the New Millennium Edition: Mainly Mechanics, Radiation, and Heat, 1. California Institute of Technology, Calfornia.
International Atomic Energy Agency, 2012. Quality Assurance Programme for Computed Tomography: Diagnostic and Therapy Application. IEA, Rep, Vienna a19.
Jursinic, P A, 2007. Characterization of optically stimulated luminescent dosimeters, OSLDs, for clinical dosimetric measurements. Med. Phys. 34 (12), 4594–4604.
Landauer, 2012. InLight microStar system user manual.. Landauer Inc..
McKeever, S W, Moscovitch, M, 2002. On the advantages and disadvantages of optically stimulated luminescence dosimetry and thermoluminescence dosimetry. Radiat. Protect. Dosim. 104 (3), 263–270.
Ministry of Health Malaysia, 2015. Technical Quality Control Protocol Handbook for Computed Tomography System.
Mutic, S, Palta, J R, Butker, E K, Das, I J, Huq, M S, Loo, L N D, Van Dyk, J, 2003. Quality Assurance for Computed-tomography Simulators and the Computed-tomography-simulation Process: Report of the AAPM Radiation Therapy Committee Task Group No. 66.
Nagel, H D, 2007. CT Parameters that Influence the Radiation Dose. Radiation Dose from Adult and Pediatric Multidetector Computed Tomography. Springer, pp. 51–79.
Pearce, M S, Salotti, J A, Little, M P, McHugh, K, Lee, C, Kim, K P, Parker, L, 2012. Radiation exposure from CT scans in childhood and subsequent risk of leukaemia and brain tumours: a retrospective cohort study. Lancet 380 (9840), 499–505.
Xu, X G, Eckerman, K F (Eds.), 2009. Handbook of Anatomical Models for Radiation Dosimetry. CRC press.
Yahnke, C J, 2009. Calibrating the microStar. Rev.2. Landauer.